Volume 1 | Number 1 | Jan 2013 | Pages 1–100

Journal of
Materials Chemistry B

Materials for biology and medicine
www.rsc.org/materialsB

ROYAL SOCIETY
OF CHEMISTRY

ROYAL SOCIETY
OF CHEMISTRY

www.rsc.org/materialsB

Multivalency: Influence of the Residence Time and the Retraction Rate on Rupture Forces Measured by AFM

Jalal Bacharouche[1, 2], Mélissa Degardin[3], Loïc Jierry[4], Cédric Carteret[1, 2], Philippe Lavalle[5, 6], Joseph Hemmerlé[4, 5], Bernard Senger[4, 5], Rachel Auzély-Velty[7], Fouzia Boulmedais[4], Didier Boturyn[3], Liliane Coche-Guérente[3], Pierre Schaaf[4, 5]and Grégory Francius[1, 2*]

[1] Université de Lorraine, Laboratoire de Chimie Physique et Microbiologie pour l'Environnement, LCPME, UMR 7564, Villers-lès-Nancy, F-54600, France.

[2] CNRS, Laboratoire de Chimie Physique et Microbiologie pour l'Environnement, LCPME, UMR 7564, Villers-lès-Nancy, F-54600, France.

[3] Université Grenoble Alpes, Département de Chimie Moléculaire, DCM, UMR5250, Grenoble, F-38000, France

[4] Centre National de la Recherche Scientifique, Unité Propre de Recherche 22, Institut Charles Sadron, Strasbourg Cedex 2, F-67034, France.

[5] Institut National de la Santé et de la Recherche Médicale, INSERM Unité 1121, Strasbourg Cedex, F-67085, France.

[6] Université de Strasbourg, Faculté de Chirurgie Dentaire, Strasbourg, F-67000, France.

[7] Université Grenoble Alpes, CERMAV-CNRS, Institut de Chimie Moléculaire de Grenoble, Grenoble Cedex 9, F-38041, France.

* Corresponding author:

Email: gregory.francius@univ-lorraine.fr

Phone: +33 (0)3 83 68 52 36

1

Abstract

The Bell-Evans theory relative to rupture forces between non-covalently interacting molecules predicts that the rupture force increases linearly with the logarithm of the force loading rate. Here we investigate by force spectroscopy performed with an atomic force microscope (AFM) the rupture forces between surfaces covered by β-cyclodextrin (β-CD) molecules and AFM tips coated with adamantane (AD) groups. The β-CD molecules are either deposited through a self-assembled monolayer (SAM) or grafted on poly(allylamine hydrochloride) chains (PAH-CD) that are adsorbed on the substrate. The AD groups are fixed covalently on the AFM tip through either a one-AD or a four-AD platform linked to the tip though a PEO chain. It is found that while the rupture forces between AFM tips covered with tetravalent AD molecules and SAM-CD surfaces do not exceed twice those found with tips covered by monovalent AD molecules, the rupture forces increase by a factor of 20 on PAH-CD substrates for a tetravalent AD covered tip compared to a monovalent one.Thus, there seems to exist a synergistic effect between the molecule multivalence and the polymeric nature of the CD-covered substrate. As found in the literature, we observe an increase of the intensity of the rupture forces between the AD-covered AFM tip and the β-CD covered substrate with the contact time over timescales up to several seconds. Finally, we find that when the host-guest system involves the multivalency of the AD guest and/or the polymeric nature of the host the mean rupture force decreases with the loading rate in contrast to what is predicted by the Bell-Evans theory. We tentatively explain this "anti-Bell-Evans" behavior by the possibility of rebinding during the rupture process. This effect should have important implications in the understanding of forces at the cellular level.

1. Introduction

Ligand/receptor interactions play a fundamental role in biology. The investigation of these interactions has attracted a tremendous amount of work. Yet, these interactions do usually not act at the single ligand/receptor level but rather act collectively: simultaneously, several ligands interact with several receptors over a constrained geometrical area. This naturally introduces the concept of multivalency. The understanding of multivalent interactions at interfaces is thus of primary importance to better understand and control biological recognition events.[1] It also provides a tool to develop supramolecular nanomaterials.[2]Nature uses multivalency to finely tune the interactions between cells and their environment because it greatly enhances the adhesion selectivity with respect to ligand or receptor density.[3] It also allows reaching very strong adhesion and irreversible adsorption with reversible interactions.

Multivalency can be studied either from a collective point of view where surfaces covered by ligands are brought in contact with solutions of receptor molecules. This allows getting access to thermodynamic or kinetic parameters characterizing the interactions. It can also be investigated from a more mechanistically point of view by force spectroscopy using an atomic force microscope (AFM) or optical tweezers. Then one gets access to information about the binding and unbinding mechanisms when the ligand/receptor complexes are under the influence of external mechanical forces. This information is of great interest to better understand how cells sense their environment and how they adhere to substrates. Here we are interested in getting new information along this line and in particular on how parameters such as the contact time between a ligand substrate and the receptor covered AFM tip or the retraction rate of an AFM tip from the contacting substrate influences the rupture forces for multivalent systems.

For a single ligand/receptor interaction both the binding and the unbinding processes correspond to diffusion processes over an energy barrier. The application of a mechanical

force on the ligand/receptor complex then leads to the diffusion over an energy barrier that is modified (especially lowered) by the force. This description was introduced by Bell[4] and further developed by Evans[5] and corresponds to the Bell-Evans theory. It predicts in particular that the rupture force between a ligand and a receptor increases when the retraction rate is increased.[4, 5] This prediction has been widely verified experimentally.

Fundamental studies of non-covalent ligand/receptor interactions have led to the development of model systems. Self-assembled monolayers (SAMs) of alkanethiolates[6, 7] on gold substrates have become ideal model systems for this purpose. The possibility of introducing functional groups makes them even more attractive for the modification of surface properties that include characterization of interactions between biomolecules and cell surface receptors, protein electron transfer, biosensing and others.[8-11] β-cyclodextrin (β-CD) terminated SAMs constitute an interesting example of receptors covalently attached to a gold substrate providing an ordered array of receptors that can bind guest molecules through multivalent interactions.[12] During the last few years great attention has been focused on β-CD guest recognition systems due to their potential applications in pharmaceutical sciences, the absence of harmful effects on human health, and because they represent a good model for receptor molecules.[13-17] β-CD is a oligosaccharide composed of seven glucose moieties linked via α(1-4) glucosidic bonds.[18, 19] These glucose-based macrocycles possess a hydrophobic cavity that enables the complexation/decomplexation of organic guests in aqueous solution.[20] This binding specificity (*i.e.* complexation/decomplexation) depends mainly on guest size and geometry due to the fact that it has to fit into the tubular cavity with a diameter of 4.7−8.3 Å.[21] Non-covalent forces such as hydrogen bonding, van der Waals interactions and hydrophobic forces are responsible for the binding specificity of these inclusion complexes.[22] A well-studied example of host-guest complex involves the β-cyclodextrin-ferrocene complex in an aqueous medium. The ferrocene moieties decomplex and rebind

spontaneously many times during the recording of an AFM force-distance curve as long as the tip stays in close proximity to the β-CD SAM.[23] Another guest molecule whose interaction with β-CD has been extensively studied is adamantane (AD). Gomez-Casado *et al*. investigated the interaction between mono-, bi- and trivalent AD molecules linked to AFM tips through small ethylene oxide chains.[24] The substrate was covered by β-CD cavities that were highly oriented and organized on the surface. These authors found that the rupture force is independent of the loading rate for monovalent AD molecules while it increases with the loading for bi- and trivalent AD molecules in a manner that is compatible with the Bell-Evans theory. They also found that the rupture force for the bi- and trivalent molecules are less than twice or thrice that of monovalent AD. These results confirmed other studies on concanavalin A/mannose[25, 26] and MUC1 antigen/antibody[27] which concluded that the rupture force scaled sublinearly with the number of bonds.[27] On the other hand a study on interactions between C60 and porphyrin derivatives concluded to a rupture force for a divalent bond that is larger than twice that of a monovalent bond.[28] In all these studies the rupture force increases with the loading rate in a manner that is compatible with the Bell-Evans theory.

Another model surface for investigating non-covalent ligand/receptor interactions is provided by polymers bearing the ligands and that are adsorbed on a substrate. In this case the substrate becomes soft and the ligands should be much more mobile than on SAMs. The effect of multivalency of host-guest interactions at polymeric interfaces has been by far less investigated than on "hard" substrates such as on SAMs. A polymeric coating may be called a "3D coating" in opposition to the 2D SAMs. The striking difference resides in the spatial distribution of the CDs either grafted on the SAMs or on the polymer. This feature is highlighted when the AZFM tip approaches from the surface. When several ADs are bound to the tip surface (not only to its apex) and are therefore differently spaced from the gold surface, even the most distant ADs may find a CD partner in the thick polymeric coating while more

rarely on the flat SAM-CD coating. The SAM-CD(NP) case is in-between with its aggregates spread over the surface. By investigating the rupture between AFM tips covered by chitosan chains onto which are grafted AD moieties and substrates covered by chitosan chains onto which are grafted β-CDs, Kaftan *et al.* found that the rupture forces increase with the contact time over timespans of several seconds.[29] The distance at which the ruptures took place largely exceeded rupture distances found on "hard" substrates for host-guest interactions. Takemasa *et al*. investigated the interaction between two polymers namely hydroxyethylcellulose and amylose.[30] They found that this system follows the Bell-Evans prediction about the evolution of the rupture force with the retraction rate but they did not focus on the influence of the contact time.

In order to gain further insight into these rupture processes we focus here on the comparison between mono- and tetravalent guest molecules interacting with host molecules located either on the substrate within SAMs or in a mess of polymer chains. For this purpose, we use cyclodecapeptide scaffolds that were already exploited to design multivalent architectures.[31] These macromolecular systems present in a spatially controlled manner two independent functional domains. [32, 33] Cyclodecapeptide scaffolds have been extremely useful in synthetic protein design and have become a versatile tool in the field of peptide mimicry[34-36] as well as for the targeted-drug delivery and for molecular imaging of tumors.[37, 38] Interestingly, they have also been used for the design of nanometer scale redox active biomolecular architecture by using ferrocenyl units.[39] In this work we provide a comprehensive study of (i) the specific binding, (ii) the influence of the residence time (*i.e.* contact time), (iii) the influence of the retraction rate on the host-guest rupture forces between a cyclodecapeptide scaffold bearing a monovalent or a tetravalent adamantyl (guest) and two types of β-CD (host) covered substrates. We use AFM force spectroscopy for this purpose. The first substrate consists of a self-assembled monolayer (SAM) of alkanethiol (p.4 "alkanethiolates"; quel est le mot

correct?) β-cyclodextrin whereas the second is a monolayer of a linear polyelectrolyte, poly(allylamine hydrochloride), onto which are grafted β-CD units resulting in (PAH-CD), both adsorbed onto gold substrates. As already discussed, the PAH-CD substrate is of great interest because the polymer provides a "soft" layer and gives higher mobility for the β-CD units grafted therein as compared to the "rigid" SAM-CD layer where the β-CD mobility is limited to rotation and bending/rocking along the axis of the alkyl chain.

2. Materials and Methods

2.1. Synthesis of the mono- and tetra-adamantane derivatives and the glycosylated polyelectrolyte PAH-CD

β-cyclodextrin (noted as β-CD), chloroform, ethanolamine hydrochloride, poly(allylamine hydrochloride) (noted as PAH, Mw~70000), dimethylsulfoxyde (noted as DMSO), tris(hydroxymethyl)aminomethane (Tris), NaCl, NaCNBH$_3$, and absolute ethanol were all purchased from Sigma-Aldrich, France. All reagents were used without further purification. HS-C$_{11}$H$_{22}$-EG$_4$-OH was purchased from Prochimia Surfaces (ProChimia Surfaces, Sopot, Poland). For AFM-tip functionalization, the PEG linkers were purchased from Hermann Gruber group (Institute of Biophysics, University of Linz, Austria).[40]

AD derivatives that incorporate one or four AD moieties were prepared by using a modular strategy. Cyclodecapeptides encompassing one or four alkyne functional groups were prepared through a solid phase peptide synthesis using aFmoc/*t*-Bu strategy with a subsequent cyclisation under high dilution in solution, according to methods previously described (See supplementary information).[41] A pegylated linker featuring an amino group was introduced by peptidic coupling on the lysine residue lateral chain of the scaffold. The grafting of azide-containing AD residues was achieved by using copper(I)-catalyzed alkyne–azide cycloaddition as outlined in Scheme 1. Adamantyl azido fragment AD-EG$_4$-N$_3$, previously

prepared by reaction of 1-adamantylamine on N_3-EG_4-NHS, was condensed on scaffolds **1** and **2** in the presence of $CuSO_4$, tris(3-hydroxypropyltriazolylmethyl)amine (THPTA) and sodium ascorbate in a degassed DMF/phosphate buffer (pH 7.4) mixture heated at 45°C for 2h30.[42] Preparative RP-HPLC afforded pure adamantyl derivatives 3 or 4, called scaffolds, in good yields, respectively 72% and 68%. In parallel, β-CD thiol synthesis was carried out by condensation of 6-monodeoxy-6-monoamino-β-cyclodextrin on commercially available HS-$C_{11}H_{22}$-EG_6-COONHS (Prochimia-Poland) in the presence of DIPEA (pH 8-9) in DMF. RP-HPLC afforded pure HS-$C_{11}H_{22}$-EG_6-CD in 42% yield (see Figure S1).

The PAH-CD has been prepared according to a described procedure[12]: β-cyclodextrin modified with an aldehyde group on the primary face[43] is brought in contact with PAH, and then reductive amination is performed leading to PAH-CD (grafting ratio of 8%).

2.2. Preparation of surfaces and AFM tips

Gold-coated glass substrates were obtained by means of a sputter coater (EMITECH, K575 Turbo, United Kingdom). The glass substrates (20 × 10 × 1 mm) were coated with a 20-nm thick chromium layer and a topmost 60-nm gold layer. Gold-coated glass substrates were cleaned with chloroform for 10 min, dried with nitrogen, and then placed into a UV−ozone cleaner (PSD UV4, Novascan Technologies Inc. Ames, IA) for 30 min. The one side of the gold substrates was brought in contact with a solution of 1mM (HS-$C_{11}H_{22}$-EG_4-OH / HS-$C_{11}H_{22}$-EG_4-CONH-CD) (7:3) either in an ethanol:water (9:1) mixture or in pure ethanol for 14 h. Two batches of HS-$C_{11}H_{22}$-EG_4-CONH-CD, one highly hydrated (solubilized in the ethanol:water mixture) and the other highly dried (solubilized in pure ethanol) were used in this study and the resulting monolayers were denoted SAM-CD(NP) and SAM-CD, respectively. The samples were extensively rinsed 10 min twice with ethanol and finally stored in absolute ethanol at 4°C (Figure 1a). Before each experiment, the samples were dried

with nitrogen and placed into the environmental closed fluid cell of the AFM containing 4mL

of a Tris/NaCl buffer solution thermostated at 37°C.

For AFM force spectroscopy experiments, AFM tips were functionalized with the selected

cyclodecapeptide scaffold (Figure 1b) *via* a 6-nmlong polyethylene glycol (PEG) chain using

a previously described protocol.[44, 45] Cantilevers were washed with chloroform and ethanol,

placed in a UV-ozonecleaner for 30 min, and incubated overnight in a DMSOsolution of

ethanolamine hydrochloride (3.3 g in 6 mL) to generate amino groups on the tip surface.[46]

These amino groups were reacted with PEG linkers carrying benzaldehyde functions on their

free-tangling end, as described elsewhere.[47] For the coupling of the scaffold, the cantilever

was covered with a 200 µL droplet of milli-Q water containing the selected scaffold at 0.1

mg/mL to which 2 µL of a 1 M $NaCNBH_3$ solution was added. After 50 min of incubation, 5

µL of an aqueous 1 M ethanolamine hydrochloride solution (pH 9.5) were added in order to

deactivate the unreacted aldehyde groups during another 10 min incubation time, after which

the cantilever was washed with and stored in the Tris/NaCl solution buffer at 4°C.

2.3. Infrared Reflection AbsorptionSpectroscopy (IRRAS)

The IRRAS spectra were recorded in the mid-infrared range on a Fourier transform infrared

spectrometer Nicolet 8700 apparatus equipped with a KBr beamsplitter and a MCT detector.

An advanced grazing angle specular reflectance accessory (Pike technologies Inc.) with a

fixed angle of incidence of 80° was used for acquiring spectra of the gold-coated surfaces.

The spectra resolution was 4 cm^{-1} and the accumulation time was 2 min. Compartments

containing the detector and the specular reflectance accessory were purged by circulating dry

N_2. IR absorbance spectra were obtained between 4000 and 600 cm^{-1}. Note that samples were

extensively rinsed with milli-Q water and then dry with dry N_2 before to be introduced in the

spectrophotometer. A total of 200 scans were performed for each sample, and the resolution was set at 4 cm^{-1}.

2.4. AFM imaging

AFM images were carried out in contact mode in aqueous medium using an MFP3D-BIO instrument (Asylum Research Technology, Atomic Force F&E GmbH, Mannheim, Germany). Silicon nitride cantilevers of conical shape were purchased from Bruker (MLCT-AU, Bruker-nano AXS, Palaiseau, France) and their low spring constants determined using the thermal calibration method, providing values of about 12-14 pN/nm. The applied force between the tip and the surface was carefully monitored and minimized at about 250 pN and all images were collected with a resolution of 512 × 512 pixels and a scan rate of 1Hz. These experimental conditions are necessary to prevent mechanical damages of the sample surface due to the lateral scanning and the corresponding shear stress.

2.5. AFM force spectroscopy and data processing

Adhesives properties of the surface samples were measured by recording Force-Volume Images (FVI) consisting of grids of 32×32 force curves obtained upon approach and subsequent retraction of the tip.Force spectroscopy measurements were performed in triplicates at 3 different locations of the sample surface corresponding to scan areas of 10 μm × 10 μm. Experiments were performed in Tris/NaCl buffer at 37°C using a constant approach and retraction speed of 1000 nm/s, various residence (contact) times in the range of 0.1-10s and a maximum applied force of 250 pN. The molecular assembly located on the sample surface was investigated upon removal of the chemically modified AFM tip away from the surface. The force curves were analyzed with a Matlab® algorithm described elsewhere.[48] This automated data processing allows the calculation of the rupture forces and the number of

adhesive events for each force curve. All FVI were analyzed with this algorithm leading to the

distribution of the rupture forces and of the adhesive events observed on 1024 retrace curves

per 10 μm × 10 μm area.

3. Results and discussion

3.1. Morphological and chemical analysis of the molecular assemblies

To investigate the effect of multivalency on host-guest interactions, two types of substrates

were covered by CD cavities and the AFM tips were functionalized with two types of

molecules bearing either one adamantane moiety (1AD) or four adamantane moieties (4AD),

corresponding respectively to the monovalent scaffold and the tetravalent scaffold. The β-CD

cavities were either deposited on a gold coating as a self-assembled monolayer or grafted onto

poly(allylamine hydrochloride) chains (PAH-CD) which were adsorbed onto the gold

substrate. Because the molecules used for the SAMs buildup presented some solubility

difficulties, we tried two deposition conditions for the SAMs: the molecules were either

dissolved in pure ethanol or in a (90:10) mixture of (ethanol:water). Using these solutions, we

followed the SAM buildup procedure described in the Materials and Methods section. The

resulting SAMs were imaged by AFM in the liquid state. Typical images are shown in Figure

2. When the SAM is formed from molecules dissolved in pure ethanol, the surface is very

homogeneous and smooth (roughness of the order of 3.2 nm) whereas when the film is

formed from a (ethanol:water) mixture the surface is covered with a film seeded by

nanoaggregates (we will call this film SAM-CD(NP)). These aggregates are very

homogeneous in size with a diameter of 125 ± 25 nm and their number density is of the order

of 10 μm^{-2}. Similar structures were already reported for thiophene-containing dextran and

cyclodextrin derivatives grafted on gold surfaces. They could originate from the self-

aggregation of β-CD either in solution or on the surface after deposition as already described

in the literature.[49] We also imaged by AFM the film resulting from the adsorption of PAH-CD

on the gold substrate (Figure 2c). This film appears much rougher (roughness of the order of

10 nm) than the SAM-CD samples and covers totally the surface.

These films were also characterized by IRRAS. Figure 3a shows the IRRAS spectra of the

SAM-CD(NP) and the SAM-CD, as well as of a SAM-OH obtained by adsorption of an

alkanethiol-PEG-OH, taken as a reference. Typical absorption bands from the β-CD were

identified at 853, 945, 1029, 1079, 1156, 1411, 1630, 2927 and 3392 cm^{-1} respectively for the

SAM-CD(NP) and SAM-CD substrates. These typical values and their corresponding

assignments have been detailed by Vico et $al.$[50] The only difference between the SAM-

CD(NP) and SAM-CD spectra is a pronounced band at 1260 cm^{-1} which is observed in the

case of the SAM-CD(NP) substrate. This difference can be related to the nano-aggregates

observed in AFM. Vico et $al.$ assessed that the appearance of the intense absorption band at

1260 cm^{-1}resulted from the clustering of β-CD molecules, with a perpendicular orientation of

their cavity axis with respect to the surface, due to hydrogen bonds (the authors noticed that

the band is not found in the solid powder). Consequently, the absence of such absorption band

in the IRRAS spectra of the SAM-CD monolayer could be related to some degree of

randomness of the orientation of the β-CD. Moreover, because part of the β-CD rings can

exhibit parallel orientation of their cavity axis with respect to the surface (Figure 4), this

orientation may support some facing interactions between the β-CD. The resulting steric

hindrance delays or even prevents the specific host-guest interactions with the adamantyl

groups. Conversely, when the plane of the β-CD cavities is oriented alongside with the

monolayer plane, the configuration is more favorable to specific host-guest interactions.

We also recorded the spectrum of the SAM-OH as a reference. It is characterized by the C-O-

C stretching band at 1120 cm^{-1}, the C-H scissoring and bending vibrations in the range of

1300-1450 cm^{-1} and the O-H stretching band at 3200 cm^{-1}. These specific absorption bands

are also detected in both the SAM-CD(NP) and the SAM-CD spectra. Figure 3b shows the

infrared spectra of the PAH-CD surface and the SAM-CD samples. The spectrum of the PAH-

CD layer was recorded under the same conditions as that of the SAM-CD surface and

indicates a more intense absorbance. This could be attributed to a higher concentration ofβ-

CD per unit area in the case of PAH-CD. This is expected since this film is assumed to be

much thicker than the SAM-CD as suggested by its much higher roughness. Some typical

absorption bands of PAH are clearly identified such as the broad absorption band associated

with the stretching mode of the NH_2 group in the range of 2800-3250 cm^{-1}. Other absorption

bands observed at 995, 1032, 1205 and 1440 cm^{-1} are in good agreement with infrared spectra

of PAH-β-CD reported in the literature.[51] From these spectra it comes out that CD moieties

are in all cases present on the surface and that they are present at a larger surface

concentration in the case of a PAH-CD than in the case of SAM-CD and SAM-CD(NP).

3.2. Comparison of the behavior of the different substrates at a fixed contact time and a

fixed retraction rate

Force curves were recorded during the retraction of the AFM tips functionalized with 1AD-

and 4AD-molecules from the substrates covered with SAM-CD(NP), SAM-CD or PAH-CD.

These curves were analyzed as reported in Figure S2 in order to quantify the rupture forces

and their corresponding statistical distributions. We define the adhesion force as the force

corresponding to the last rupture during a retraction process. We first verified the specificity

of the AFM tips to β-CD by performing force measurements on bare gold surfaces and on the

SAM-OH substrate. No significant interactions were detected on both substrates, *i.e.* more

than 80-85% of the retraction curves showed no adhesion, the remaining force curves

showing adhesive events characterized by a rupture force lower than 50 pN (Figure S3). This

small amount of weak adhesive events is related to non-specific interactions between the tip

and the substrate. Typical retraction curves for each substrate are represented in Figure 5 for a contact time between the tip and the substrate of 1s and a retraction rate of 1000 nm/s. The results are summarized in Table 1. Before examining this table in detail, it may be worth noting that the adhesion force, the adhesion frequency and the corresponding rupture length are invariably in the order SAM-CD < SAM-CD(NP) ≤ PAH-CD, whatever the valence of the guest molecules and whatever the nature of the guest-bearing coating.

a) 1AD-guest molecules

One first observes that for AFM tips functionalized with 1AD molecules, the intensity of the mean rupture forces lies always in the range 60-220 pN. These values are in line with previous works performed by others on cyclodextrin/adamantane systems where adhesion forces in the range 80-180 pN have been reported.[24] Moreover, the range of 60-220 pN is specific of host-guest interactions measured on other system such as ferrocene/β-CD or lectin/carbohydrate.[18, 52, 53]

More precisely, a mean adhesion force of the order of 200 pN is measured on SAM-CD(NP) and on PAH-CD whereas on SAM-CD it is of the order of 70 pN, *i.e.* 3 times smaller. The proportion of retractions leading to a last rupture force larger than 10 pN is of the order of 30% on the SAM-CD and 60% on the SAM-CD(NP) substrates and nearly 80% on a PAH-CD substrate.

These results highlight the influence of the surface topography on the host-guest interaction forces. On SAM-CD, because the cavities are oriented randomly, one can expect steric hindrance for the penetration of (adamantane+linker) molecules due to neighboring CD cavities (see sub-section 3.1). This hindrance reduces as well the frequency of binding as the strength of the bond due to a mismatch of the respective orientations of the cavity and the AD. On PAH-CD covered surfaces, this mismatch is also possible but the great orientation freedom of the CDs allows eventually an efficient connection between AD and CD and

thereby a strong bond. In addition, the 3D availability of the CDs favors the number of possible bonds especially if one reminds that several ADs are generally grafted on the tip (even in the case of 1AD-scaffolds). The case of the SAM-CD(NP) appears in some sense intermediate. The aggregates (see scheme in Fig. 4) force the CDs to orient their cavity towards the solvent (axis perpendicular to the substrate). This means that the aggregates minimize the drawback of steric hindrance. Furthermore, the aggregates form "towers" of various heights (from about 2 to 10 nm) in contrast to the "flat" CD coverage in the SAM-CD layer. This height non-uniformity makes the SAM-CD(NP) capable (to some extent as the PAH-CD) to capture ADs located at different altitudes above the surface, whence the adhesion frequency between that of the two other coatings (34 <58 < 80%). As to the adhesion force, the multiple bonds that can be formed make the host-guest separation more difficult and produce the increase of the last rupture force which is the adhesion force by design.

b) 4AD-guest molecules

Let us now focus on the experiments where the tips are covered by the 4AD scaffolds. One observes that the mean adhesion force increases only by a factor of about 2 between 1AD-tips and 4AD-tips probing SAM-CD and SAM-CD(NP) while it increases by a factor of the order of 20 on PAH-CD. As to the frequency of retraction curves leading to a measurable adhesion force, it is similar for 1AD- and 4AD-functionalized tips on SAM-CD and PAH-CD substrates. The fact that for 4AD it remains similar to that for 1AD on the PAH-CD substrate is not surprising since the frequency of ruptures is already high (80%) for 1AD-tips so that it could hardly be larger for 4AD-tips. On the other hand, the rupture frequency increases significantly on SAM-CD(NP) when using multivalent molecules instead of monovalent ones (from 60 to 80%). The probability of a measurable adhesion force becomes close to that observed on PAH-CD substrates.

It is also very instructive to analyze the mean rupture length. On SAM-CD(NP) and SAM-CD substrates the rupture lengths are larger, but remain of the same order of magnitude for tips functionalized with 4AD molecules compared to 1AD (70 nm compared to 50 nm on SAM-CD(NP) and 45 nm compared to 20 nm on SAM-CD) whereas on a PAH-CD substrate, one finds rupture lengths that are much larger: 380 nm for 4AD and 250 nm for 1AD molecules. Such large distances are not compatible with the molecular dimensions of the (linker+adamantane) molecules. They indicate that the PAH chains must follow the tip movement during the rupture event and that the PAH chains may even decrease their number of attachment points on the surface. Moreover the PAH chains must stretch during the retraction process. Our results show that this effect is much enhanced by the multivalency of the guest molecules. We will come back to this point when discussing the influence of the retraction rate on the rupture force.

In order to rationalize these results one can assume that the SAM-CD(NP) substrate behaves as a flat, though decorated with stacked CDs, hard and organized host assembly organized to have the CD openings oriented to catch the ADs. The SAM-CD substrate behaves more as a collection of isolated, randomly oriented host molecules. In contrast, the PAH-CD substrate is a soft 3D polymeric architecture grafted with mobile cavities. The higher degree of freedom of these hosts, compared to the two SAMS, favors the appearance of a multi-bond interaction with the AFM-tip. It thus comes out that there is a large synergistic effect between the substrate morphology and the guest. This shows up in the frequency of ruptures and even more in the mean intensity of the adhesion force which can increase by a factor of 20 when the hosts are fixed on polymers attached to the surface.

3.3. Effect of the contact time at a fixed retraction rate

Let us now discuss the effect of the contact time between the AFM tip and the different substrates on the rupture forces. The results are summarized in Figure 6. One observes that in all cases, the frequency of adhesive events increases with the residence time. This effect is particularly striking on SAM-CD where for a contact time of 0.1s only 20% of the retraction curves lead to an interaction and rises up to 50-60% for a contact time of 10 s. Moreover, at first sight, it is surprising that the rupture probability increases over a time span at least as long as 10 s. This increase must be related to the probability for a host molecule to find a guest molecule with which it can interact. Our results indicate that the probability of a host to encounter a guest is small on SAM-CD but much larger on PAH-CD. This is expected since on PAH-CD the CDs are much more mobile than in SAM-CD due to the mobility of the PAH chains and the possibility for the CDs to move with three degrees of freedom rather than only two for the surface-confined CDs in the SAM-CD coating. Moreover, the tip is expected to penetrate slightly in the PAH-CD layer during contact and thus to increase the probability for guest molecules to encounter CD cavities. These results also indicate that the overall dynamics of these molecules when the AFM tip is in contact with the substrate is slow. The dynamics of these processes may eventually depend upon the contact force which was held constant and equal to 250 pN in our case. Yet, even if this timescale can appear long, similar long times were reported by Kaftan *et al.* which investigated the interaction between a surface covered by chitosan bearing CD and an AFM tip coated by chitosan bearing AD groups.[29]

As far as the mean adhesion force is concerned, it is a slowly varying function of the residence time for 1AD on SAM-CD and on SAM-CD(NP) and for 4AD on SAM-CD whereas it increases steadily for 1AD on PAH-CD and for 4AD on SAM-CD(NP) and on PAH-CD. In spite of this difference, the adhesion force appears to vary as log(contact time) over the domain investigated. The results in Fig. 6 (three upper panels) indicate that the

sensitivity of the adhesion force to the contact time is magnified by the probability for a guest to bind with a host. As already evoked this probability is favored by the presence of aggregates of various heights on the SAM-CD(NP) coatings and by the CDs grafted on PAH chains which analogously can be reached at various heights above the gold substrate.

One can emphasize that such effect of the residence time on host-guest interactions has been reported in the literature for other systems. Recently, specific binding of bovine serum albumin (BSA) with lysozyme and dextran has been measured for a residence time ranging from 0.001s up to 90s. The authors evidenced an exponential increase of the adhesion forces with respect to residence time from 0.2 to 10 nN.[54] They attributed the effect of the residence time on the specific adhesion forces to two factors. The first is related to the water exclusion because during the long contact time between the tip and the surface, the water molecules are pushed out from the interacting system. The second factor resulted from the molecular rearrangement/orientation that occurred between the molecules and polymers attached to the tips and the substrate, respectively.[54] This second explanation is close to what we expect in our system.

3.4. Effect of the retraction rate at a fixed residence time

It is known since the work of Bell and Evans that the rupture process between interacting molecules is in fact a diffusion process over an energy barrier.[4, 5] The consequence of this is that the rupture force is not an intrinsic characteristic property of the interaction but depends upon the retraction rate applied to break the bond. It is predicted by the Bell-Evans theory that the rupture force increases with increasing loading rate.[5] We find this behavior on SAM-CD and SAM-CD(NP) for tips functionalized with 1AD molecules. Yet, with 4AD molecules on all substrates and with 1AD molecules on the PAH-CD substrate we observe a decrease instead of an increase of the mean rupture force when the retraction rate is increased (Figure

7). Such a decrease thus appears either when the tip bears multivalent guest molecules or when the morphology of the substrate corresponds to an increased host density. To our knowledge such a behavior has never been reported so far. It is especially striking on PAH-CD with 4AD molecules.

This effect may be tentatively explained as follows. Let us consider systems where the different individual interacting molecules (in our case the AD moieties on the 4AD-scaffold and the CD cavities on the PAH-CD chains) are mobile and elastic along the retraction direction. During the retraction process, the different AD-CD bonds will not break simultaneously but one can expect that they will break sequentially provided that the retraction velocity is not too high. This is why the intensity of the rupture force on SAM-CD is only multiplied by a factor of 2 on 4AD-functionalized tips compared to 1AD functionalized ones. When one bond breaks, due to the elasticity of the system and to the existence of remaining bonds, the tip remains in contact with the substrate and rebinding can take place. This should be particularly the case for PAH-CD where PAH chains can also gradually detach from the substrate and/or stretch so that the whole layer "follows" locally the movement of the tip (Scheme 2). This is in accordance with the large rupture lengths observed on PAH-CD. Once the bond that broke rebinds the whole individual rupture process (diffusion process over an energy barrier) will have to start again, but the applied force has increased in the meanwhile (Scheme 2). In short, our observations suggest that in the present conditions the rebinding effect dominates over the opposite Bell-Evans trend which, however, is revealed by the breaking of the bonds implying 1AD-molecules. This effect should be favored for very elastic systems (*e.g.* PAH-CD layer) interacting with highly multivalent guests such as 4AD-scaffolds. The synergy between the substrate elasticity and the multivalency of the molecules attached on the tip leads thus to the enhanced intensity of the rupture forces on the PAH-CD/4AD system seen previously. Note finally that the elasticity of

19

the PAH chains reduces the loading rate at a given retraction velocity when compared to the loading rate at the same retraction velocity when the SAM-CD and SAM-CD(NP) are concerned instead of PAH-CD. This point may appreciably alter the unbinding regime. Qualitatively, the unbinding from PAH-CD proceeds as though the PAH chain were stiff and the retraction velocity much smaller. This specific feature of the polymer layer reinforces the role of the rebinding discussed above. Note that the probability of a measurable adhesion force remains close to 60-80% over the retraction speed range for the SAM-CD(NP) and PAH-CD substrates whatever the AD scaffold. This quasi stability of the probability of adhesive events must be related to the fact that the contact time of 1 s is enough to completely achieve the AD-CD binding before AFM-tip retraction. Conversely, a weak decrease of the probability from 60 to 40% is observed on the SAM-CD substrate. This effect may be tentatively explained by the hindrance generated by both CD unfavorable cavities orientation and too important neighboring CD cavities distances.

4. Conclusions

The investigation of specific binding between mono (1AD) and tetravalent (4AD) scaffolds interacting with "hard" and polymeric substrates covered with β-CD evidenced molecular binding/rebinding processes that strongly depend on the residence time (*i.e.* contact time) and the retraction rate. The two most striking results that we observe are (i) the synergy between the multivalence of the guest molecules and the morphology of the substrate (PAH-CD) as far as the mean rupture force is concerned. We find a 20-fold increase of this force for 4AD functionalized tips compared to 1AD functionalized ones when interacting with PAH-CD; (ii) an "anti-Bell-Evans" effect for multivalent systems (in particular for 4AD on PAH-CD) characterized by a decrease of the mean rupture force when the retraction rate is increased, in contrast with the prediction of the Bell-Evans theory. This effect, never observed so far to our

knowledge, is explained by the unbinding/rebinding of β-CD during the rupture process of the tip from the substrate. All the interactions between AD and β-CD do not break simultaneously but may break sequentially in a unbinding/rebinding process. Such a mechanism must be influenced by both the elasticity of the multivalent molecules on the tip and the dynamics of the substrate. It is probably enhanced by higher flexibility, softness and mobility given by the polymeric chains.

Acknowledgments

Electronic Supplementary Information Available

Electronic Supplementary Information (ESI) available: This material is available free of charge via the Internet at http://rsc.org

References

1.   L. L. Kiessling, J. E. Gestwicki and L. E. Strong, *Angew. Chem.-Int. Edit.*, 2006, 45, 2348-2368.

2.   J. D. Badjic, A. Nelson, S. J. Cantrill, W. B. Turnbull and J. F. Stoddart, *Acc. Chem. Res.*, 2005, 38, 723-732.

3.   G. V. Dubacheva, T. Curk, B. M. Mognetti, R. Auzely-Velty, D. Frenkel and R. P. Richter, *J. Am. Chem. Soc.*, 2014, 136, 1722-1725.

4.   G. I. Bell, *Science*, 1978, 200, 618-627.

5.   E. Evans and K. Ritchie, *Biophys. J.*, 1997, 72, 1541-1555.

6.   A. Ulman, *An Introduction to Ultrathin Organic Films: From Langmuir-Blodgett to Self-Assembly*, ACADEMIC PressINC, 1991.

7.   H. O. Finklea, in *Electroanal. Chem.*, eds. A. J. Bard and I. Rubinstein, New York, 1996, vol. 19, p. 544.

8.   J. J. Gooding and S. Ciampi, *Chem. Soc. Rev.*, 2011, 40, 2704-2718.

9.   J. D. Zhang, Q. J. Chi, A. G. Hansen, P. S. Jensen, P. Salvatore and J. Ulstrup, *FEBS Lett.*, 2012, 586, 526-535.

10.   J. T. Koepsel and W. L. Murphy, *ChemBioChem*, 2012, 13, 1717-1724.

11.   D. H. Murgida and P. Hildebrandt, *Chem. Soc. Rev.*, 2008, 37, 937-945.

12.   G. V. Dubacheva, P. Dumy, R. Auzely, P. Schaaf, F. Boulmedais, L. Jierry, L. Coche-Guerente and P. Labbe, *Soft Matter*, 2010, 6, 3747-3750.

13.   J. M. Campina, A. Martins and F. Silva, *Electrochim. Acta*, 2009, 55, 90-103.

14.   J. Szejtli, *Chem. Rev.*, 1998, 98, 1743-1753.

15.   A. R. Khan, P. Forgo, K. J. Stine and V. T. D'Souza, *Chem. Rev.*, 1998, 98, 1977-1996.

16.   M. Singh, R. Sharma and U. C. Banerjee, *Biotechnol. Adv.*, 2002, 20, 341-359.

17.   K. Odashima, M. Kotato, M. Sugawara and Y. Umezawa, *Anal. Chem.*, 1993, 65, 927-936.

18.   T. Auletta, M. R. de Jong, A. Mulder, F. van Veggel, J. Huskens, D. N. Reinhoudt, S. Zou, S. Zapotoczny, H. Schonherr, G. J. Vancso and L. Kuipers, *J. Am. Chem. Soc.*, 2004, 126, 1577-1584.

19.   J. Szejtli, *Cyclodextrin Technology*, Kluwer Academic, Dordrecht, Davies, J. E. D. edn., 1988.

20.   M. R. de Jong, J. Huskens and D. N. Reinhoudt, *Chemistry-a European Journal*, 2001, 7, 4164-4170.

21.   S. Li and W. C. Purdy, *Chem. Rev.*, 1992, 92, 1457-1470.

22.   C. Henke, C. Steinem, A. Janshoff, G. Steffan, H. Luftmann, M. Sieber and H. J. Galla, *Anal. Chem.*, 1996, 68, 3158-3165.

23.   S. Zapotoczny, T. Auletta, M. R. de Jong, H. Schonherr, J. Huskens, F. van Veggel, D. N. Reinhoudt and G. J. Vancso, *Langmuir*, 2002, 18, 6988-6994.

24.   A. Gomez-Casado, H. H. Dam, M. D. Yilmaz, D. Florea, P. Jonkheijm and J. Huskens, *J. Am. Chem. Soc.*, 2011, 133, 10849-10857.

25.   T. V. Ratto, K. C. Langry, R. E. Rudd, R. L. Balhorn, M. J. Allen and M. W. McElfresh, *Biophys. J.*, 2004, 86, 2430-2437.

26.   T. V. Ratto, R. E. Rudd, K. C. Langry, R. L. Balhorn and M. W. McElfresh, *Langmuir*, 2006, 22, 1749-1757.

27.   T. A. Sulchek, R. W. Friddle, K. Langry, E. Y. Lau, H. Albrecht, T. V. Ratto, S. J. DeNardo, M. E. Colvin and A. Noy, *Proc. Natl. Acad. Sci. USA*, 2005, 102, 16638-16643.

28.   Y. H. Zhang, Y. Yu, Z. H. Jiang, H. P. Xu, Z. Q. Wang, X. Zhang, M. Oda, T. Ishizuka, D. L. Jiang, L. F. Chi and H. Fuchs, *Langmuir*, 2009, 25, 6627-6632.

29.   O. Kaftan, S. Tumbiolo, F. Dubreuil, R. Auzely-Velty, A. Fery and G. Papastavrou, *J. Phys. Chem. B*, 2011, 115, 7726-7735.

30.   M. Takemasa, M. Sletmoen and B. T. Stokke, *Langmuir*, 2009, 25, 10174-10182.

31.   D. Boturyn, E. Defrancq, G. T. Dolphin, J. Garcia, P. Labbe, O. Renaudet and P. Dumy, *J. Pept. Sci.*, 2008, 14, 224-240.

32.   P. Dumy, I. M. Eggleston, G. Esposito, S. Nicula and M. Mutter, *Biopolymers*, 1996, 39, 297-308.

33.   P. Dumy, I. M. Eggleston, S. Cervigni, U. Sila, X. Sun and M. Mutter, *Tetrahedron Lett.*, 1995, 36, 1255-1258.

34.   G. Tuchscherer, D. Grell, M. Mathieu and M. Mutter, *J. Pept. Res.*, 1999, 54, 185-194.

35.   M. Mutter and G. Tuchscherer, *Cell. Mol. Life Sci.*, 1997, 53, 851-863.

36.   G. Tuchscherer and M. Mutter, *J. Biotechnol.*, 1995, 41, 197-210.

37.   E. Garanger, D. Boturyn, J. L. Coll, M. C. Favrot and P. Dumy, *Org. Biomol. Chem.*, 2006, 4, 1958-1965.

38.   D. Boturyn, J. L. Coll, E. Garanger, M. C. Favrot and P. Dumy, *J. Am. Chem. Soc.*, 2004, 126, 5730-5739.

39. C. H. Devillers, D. Boturyn, C. Bucher, P. Dumy, P. Labbe, J. C. Moutet, G. Royal and E. Saint-Aman, *Langmuir*, 2006, 22, 8134-8143.

40. L. Wildling, B. Unterauer, R. Zhu, A. Rupprecht, T. Haselgrübler, C. Rankl, A. Ebner, D. Vater, P. Pollheimer, E. E. Pohl, P. Hinterdorfer and H. J. Gruber, *Bioconjugate Chem.*, 2011, 22, 1239-1248.

41. M. Galibert, P. Dumy and D. Boturyn, *Angew. Chem.-Int. Edit.*, 2009, 48, 2576-2579.

42. V. Hong, S. I. Presolski, C. Ma and M. G. Finn, *Angew. Chem.-Int. Edit.*, 2009, 48, 9879-9883.

43. A. Charlot, A. Heyraud, P. Guenot, M. Rinaudo and R. Auzely-Velty, *Biomacromolecules*, 2006, 7, 907-913.

44. G. Francius, D. Alsteens, V. Dupres, S. Lebeer, S. De Keersmaecker, J. Vanderleyden, H. J. Gruber and Y. F. Dufrêne, *Nat. Protoc.*, 2009, 4, 939-946.

45. G. Francius, S. Lebeer, D. Alsteens, L. Wildling, H. J. Gruber, P. Hols, S. De Keersmaecker, J. Vanderleyden and Y. F. Dufrêne, *ACS Nano*, 2008, 2, 1921-1929.

46. C. K. Riener, C. M. Stroh, A. Ebner, C. Klampfl, A. A. Gall, C. Romanin, Y. L. Lyubchenko, P. Hinterdorfer and H. J. Gruber, *Anal. Chim. Acta*, 2003, 479, 59-75.

47. A. Ebner, L. Wildling, R. Zhu, C. Rankl, T. Haselgrubler, P. Hinterdorfer and H. J. Gruber, in *Stm and Afm Studies On*, Springer-Verlag Berlin, Berlin, 2008, vol. 285, pp. 29-76.

48. P. Polyakov, C. Soussen, J. B. Duan, J. F. L. Duval, D. Brie and G. Francius, *PLoS One*, 2011, 6, e18887.

49. S. Hornig, T. Liebert, A. R. Esker, S. L. Stoll, J. Mertzman, W. G. Glasser and T. Heinze, *Langmuir*, 2009, 25, 4845-4847.

50. R. V. Vico, R. H. de Rossi and B. Maggio, *Langmuir*, 2010, 26, 8407-8413.

51. B. G. Mathapa and V. N. Paunov, *Soft Matter*, 2013, 9, 4780-4788.

52. A. Touhami, B. Hoffmann, A. Vasella, F. A. Denis and Y. F. Dufrêne, *Langmuir*, 2003, 19, 1745-1751.

53. I. V. Safenkova, A. V. Zherdev and B. B. Dzantiev, *Biochem.-Moscow*, 2012, 77, 1536-1552.

54. L. C. Xu, V. Vadillo-Rodriguez and B. E. Logan, *Langmuir*, 2005, 21, 7491-7500.

Tables

Table 1.

Average adhesion force, probability of adhesive events and the average rupture length for the interactions between 1AD (top value) and 4AD derivatives (bottom value) with the substrates containing the β-CD. Force spectroscopy experiments were performed for a retraction speed of 1000 nm/s with a contact time of 1s onto 10 μm × 10 μm surface areas in aqueous medium at 37°C. Mean values and standard errors were calculated from the analysis of 3072 force curves for each sample.

Samples	SAM-CD(NP)	SAM-CD	PAH-CD
Adhesion force (nN)	0.188 ± 0.014 0.266 ± 0.018	0.069 ± 0.008 0.132 ± 0.011	0.212 ± 0.009 3.738 ± 0.144
Frequency (%)	58.3 76.5	34.1 31.7	79.8 77.3
Rupture length (nm)	48.1 ± 1.7 67.8 ± 1.6	20.0 ± 0.7 45.9 ± 2.8	252 ± 14 378 ± 20

List of Figures
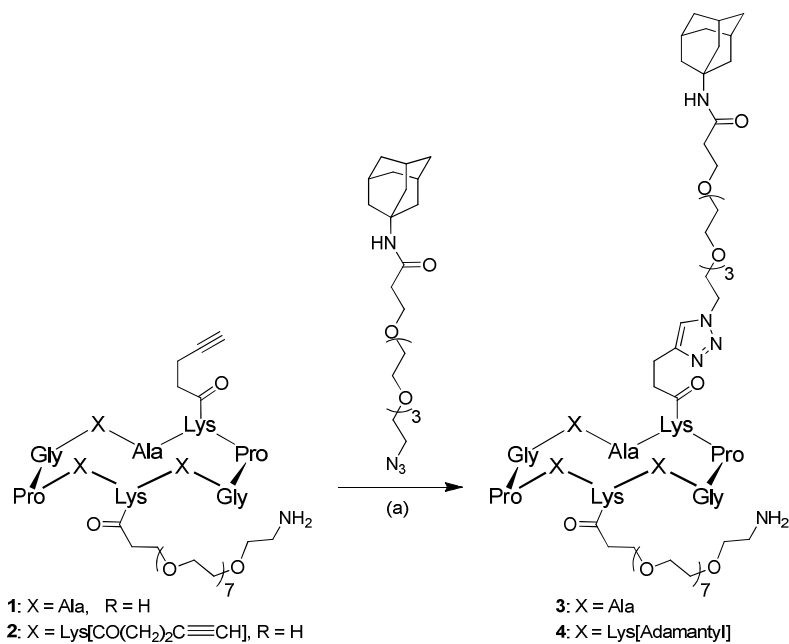
Scheme 1.

Synthesis of adamantyl featuring peptidic scaffolds **3** and **4**. *Reagents and conditions:* (a)

CuAAC: **2**, CuSO$_4$, THPTA, AscNa, Phosphate buffer pH 7.4, DMF, 45°C, 3h, **3**: 72%, **4**:

68%.
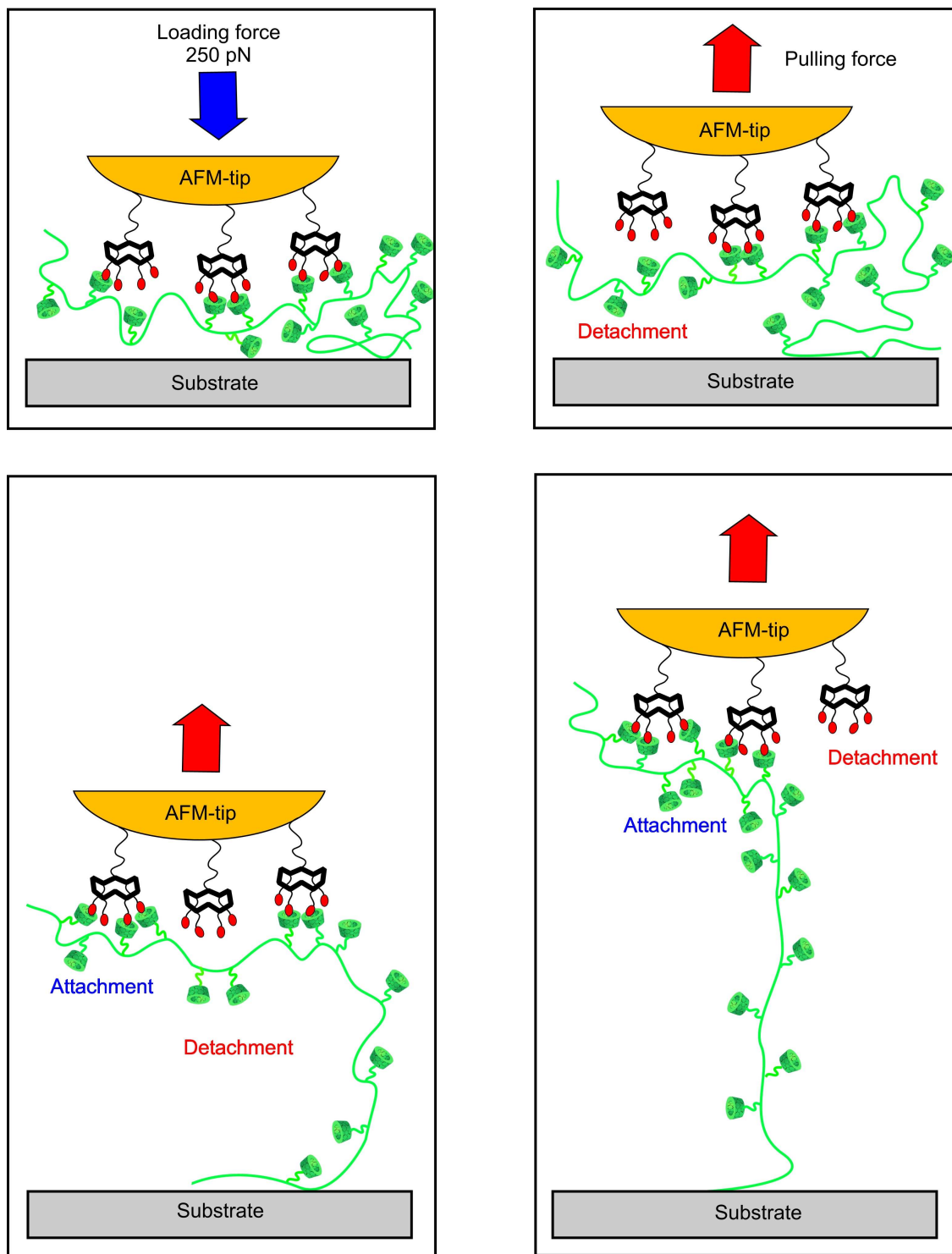
Scheme 2.

Scheme of detachment/attachment dynamics of AD derivatives from/to the β-CD grafted on a

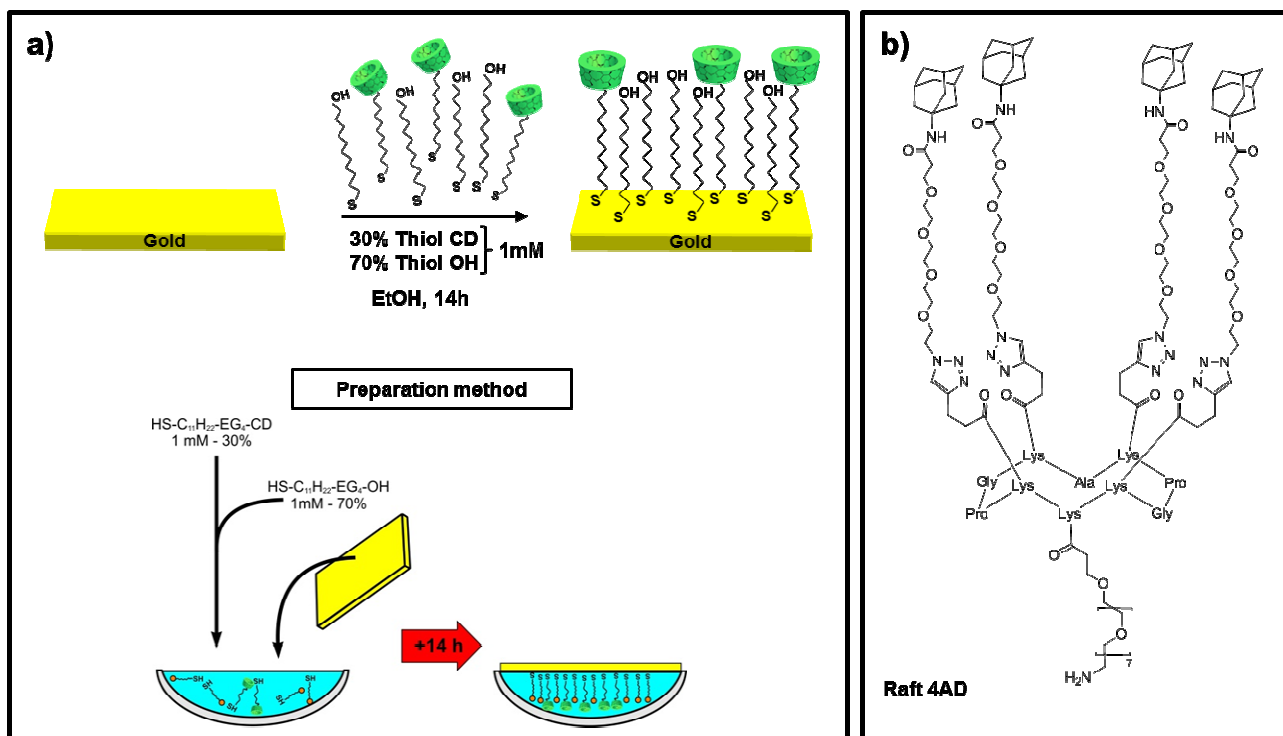PAH chain during the AFM tip retraction under low withdrawal speed.

Figure 1.

a) Scheme of the SAM-CD preparation from a mixture solution of 30% HS-C$_{11}$H$_{22}$-EG$_4$-CD and 70% HS-C$_{11}$H$_{22}$-EG$_4$-OH in ethanol. The preparation method consists of immersing for 14 h one side of the gold-coated glass substrate in a watch glass containing 2 mL of the thiol mixture. b) Chemical structure of the adamantyl scaffold containing 4 adamantyl ligands grafted onto a cyclodecapeptide platform *via* one EG$_4$ spacer.
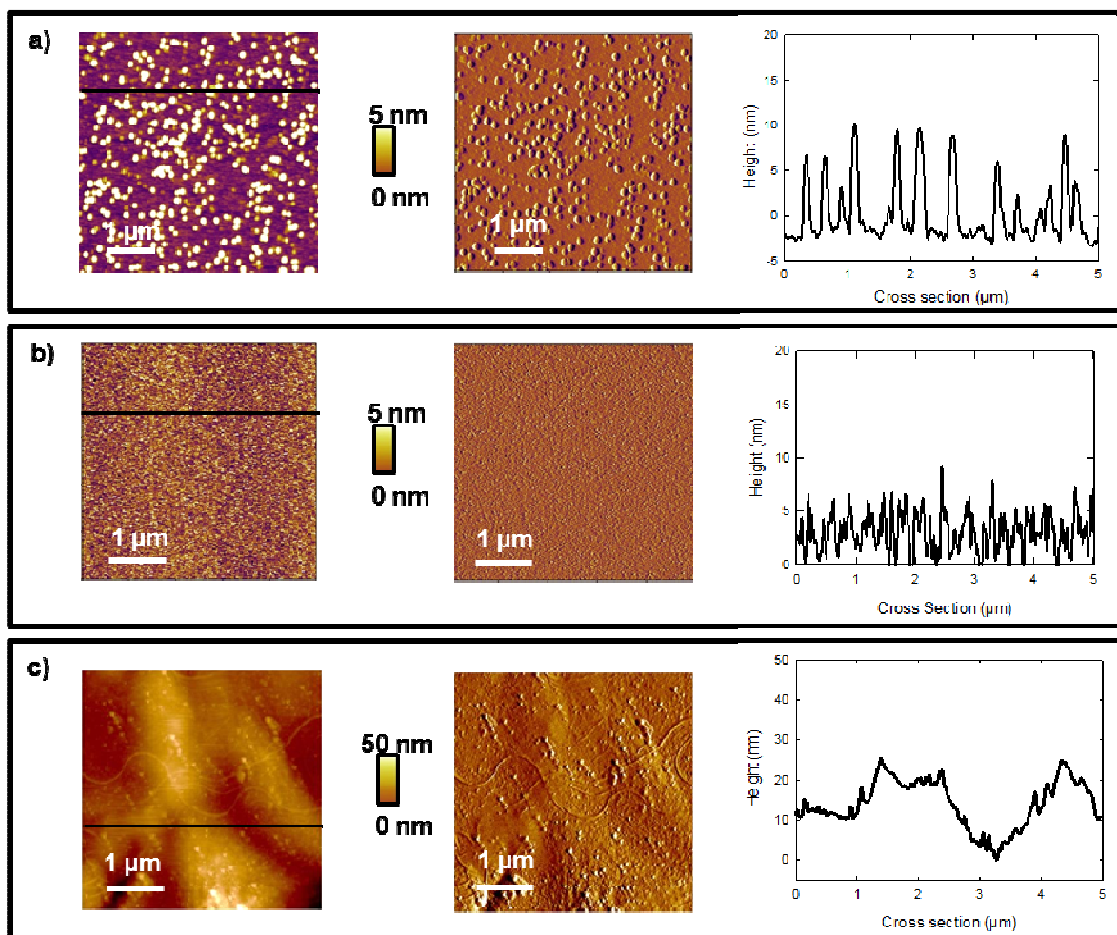
Figure 2.

a) Deflection and height AFM images recorded on a SAM-CD(NP) coated gold surface over a 5 µm × 5 µm area in aqueous medium at 37°C. The height profile on the right inset corresponds to the cross section taken along the black line. b) Deflection and height AFM images recorded on a SAM-CD coated gold surface over a 5 µm × 5 µm area in aqueous medium at 37°C. The height profile on the right inset corresponds to the cross section taken along the black line. c) Deflection and height AFM images recorded on a PAH-CD coated gold substrate over a 5 µm × 5 µm area in aqueous medium at 37°C. The height profile on the right inset corresponds to the cross section taken along the black line.

4
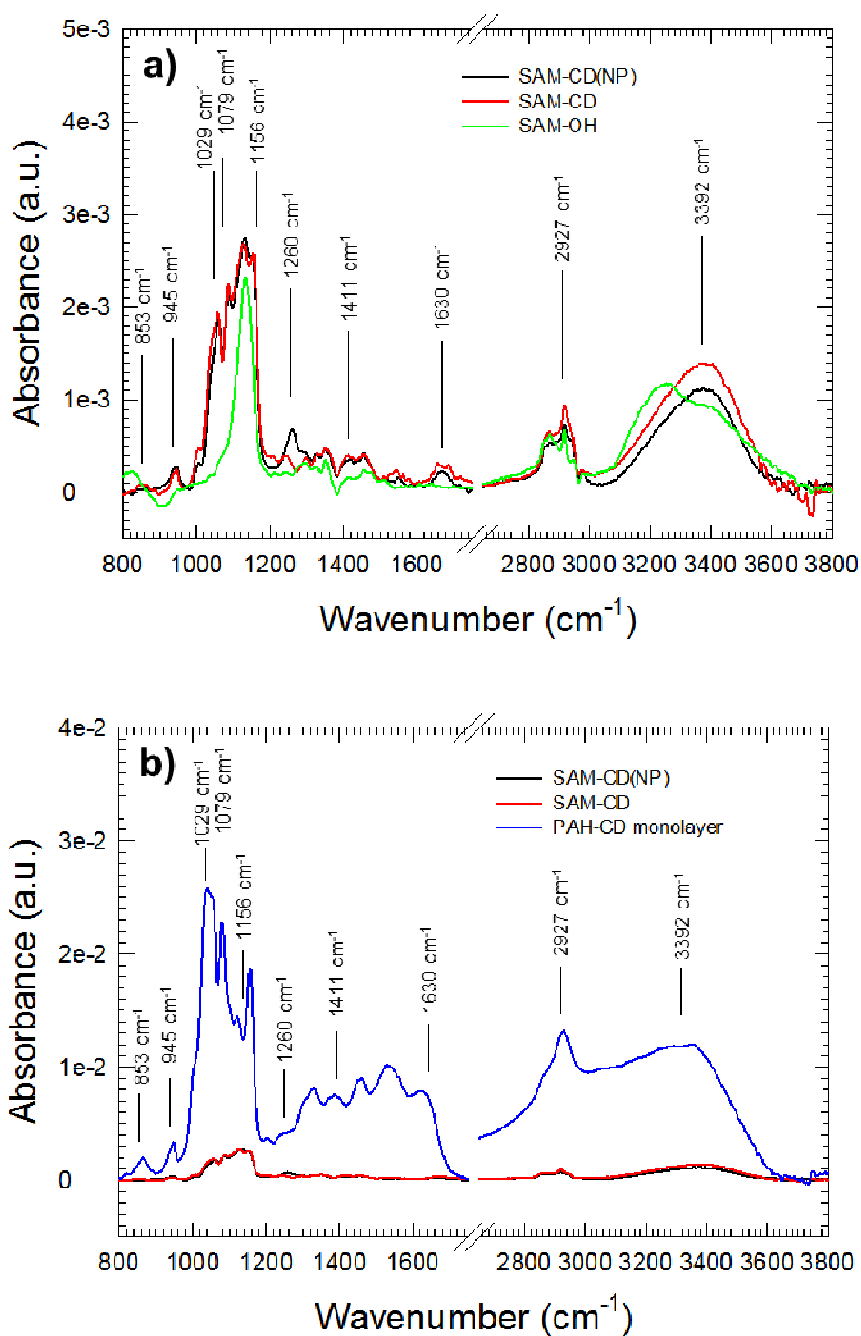
Figure 3.

a) IRRAS spectra of SAM-CD(NP) (black line), SAM-CD (red line) and SAM-OH (green line) monolayers. b) IRRAS spectra of SAM-CD(NP) (black line), SAM-CD (red line) and PAH-CD (blue line) monolayers. Note that absorbance of the PAH-CD coated substrate is 10 times larger than the absorbance of the β-CD monolayer.
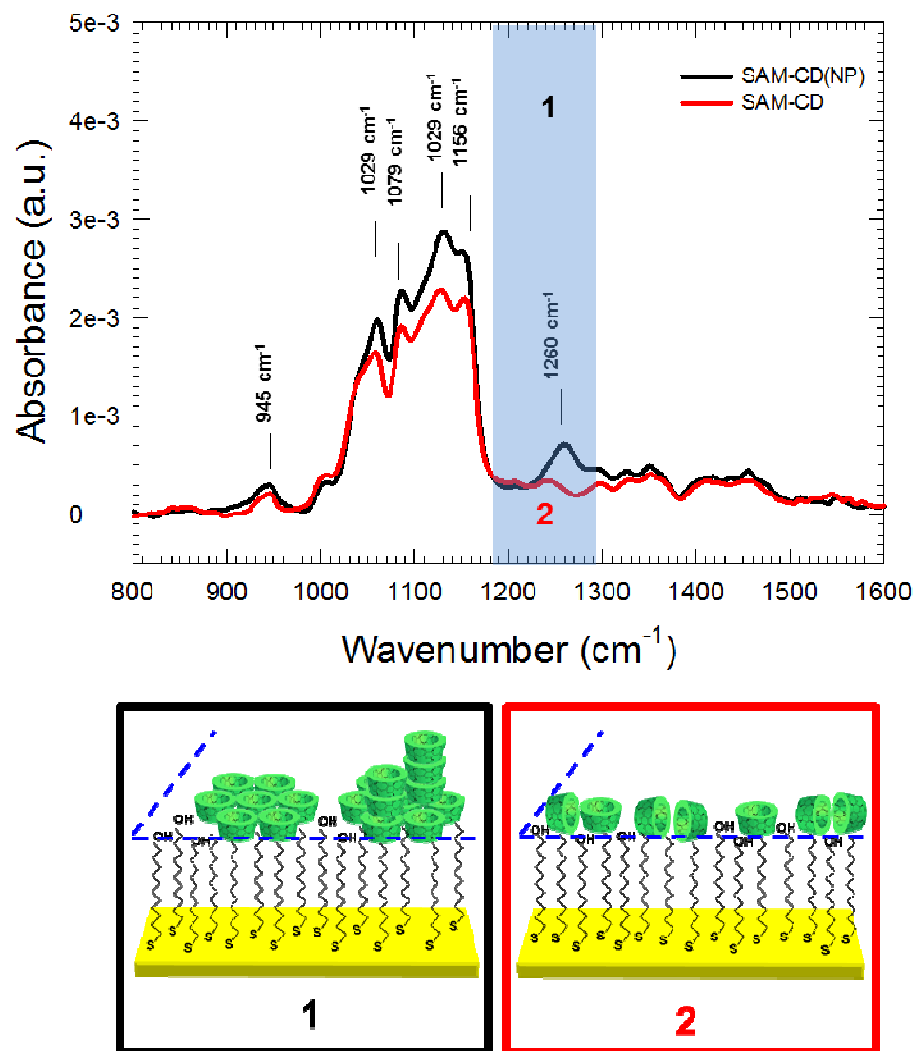
5

Figure 4.

IRRAS spectra of the SAM-CD(NP) sample (1- black line) and the SAM-CD sample (2 - red line), and the corresponding molecular orientations of the β-CD within the monolayer plane (delimited by the blue dashed lines).
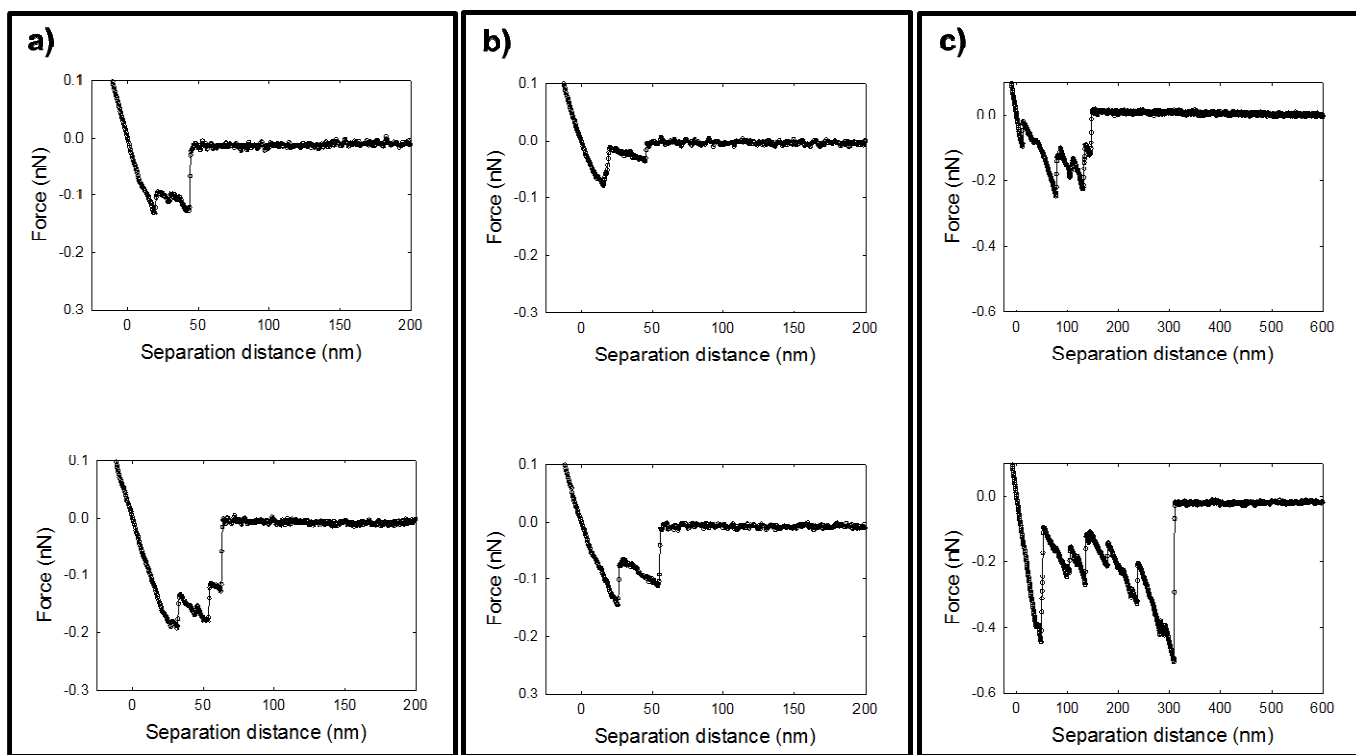
Figure 5.

Representative retraction force curves recorded during force spectroscopy measurements over a 10 µm × 10 µm surface area in aqueous medium at 37°C with the monovalent (top) and the tetravalent (bottom) adamantyl scaffold grafted on the AFM-tip. a) SAM-CD(NP); b) SAM-CD; c) PAH-CD coated on a gold substrate. All these force measurements were performed with an approach rate of 1000 nm/s, a loading force of 250 pN, a retraction rate of 1000 nm/s and a residence time of 1 s.
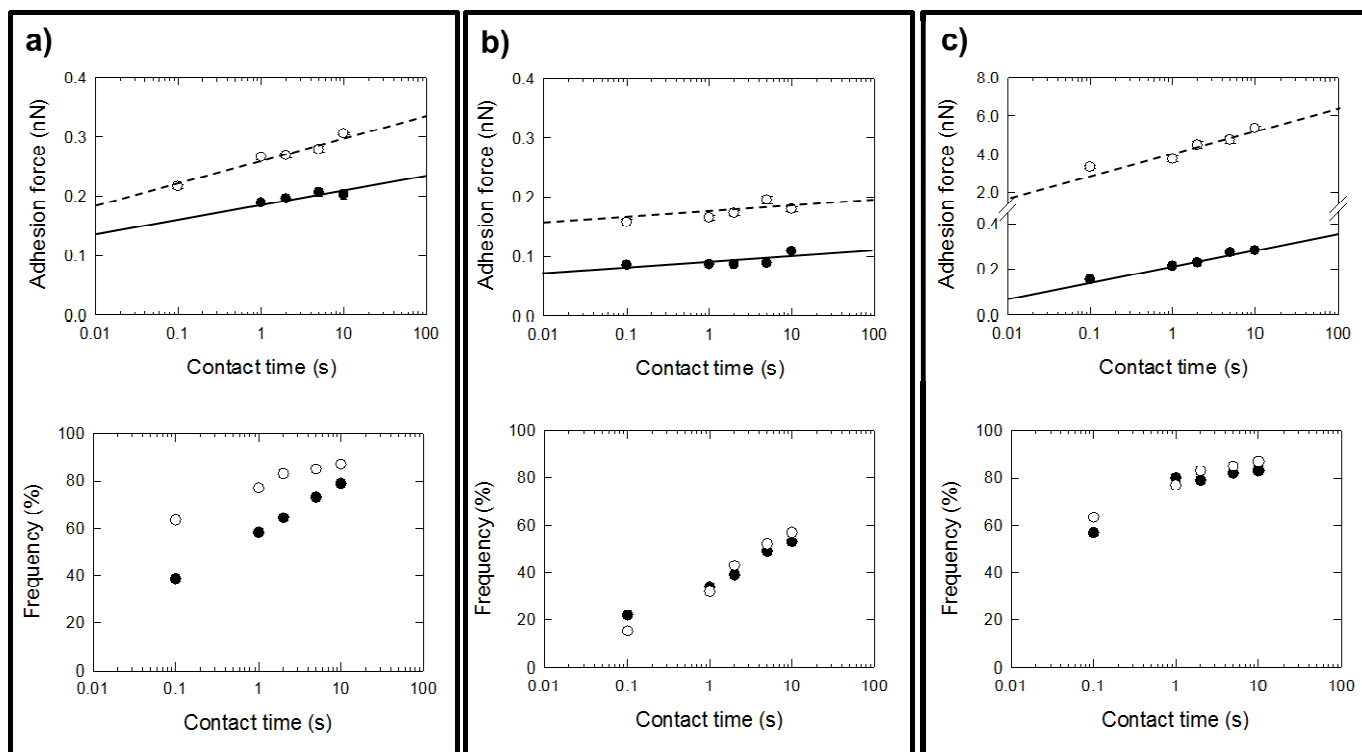
7

Figure 6.

Variations of the average adhesion force and probability of adhesive events as a function of the contact time performed by force spectroscopy onto 10 μm × 10 μm surface areas in aqueous medium at 37°C with the monovalent (black circle) and the tetravalent (white circle) adamantyl scaffold grafted on the AFM-tip. a) SAM-CD(NP); b) SAM-CD; c) PAH-CD coated on a gold substrate. Each mean value corresponds to the arithmetic mean of the non-zero forces out of the 3×1024 force curves recorded; the error bars correspond to the standard errors. All these force measurements were performed with an approach rate of 1000 nm/s, a loading force of 250 pN, and a retraction rate of 1000 nm/s.
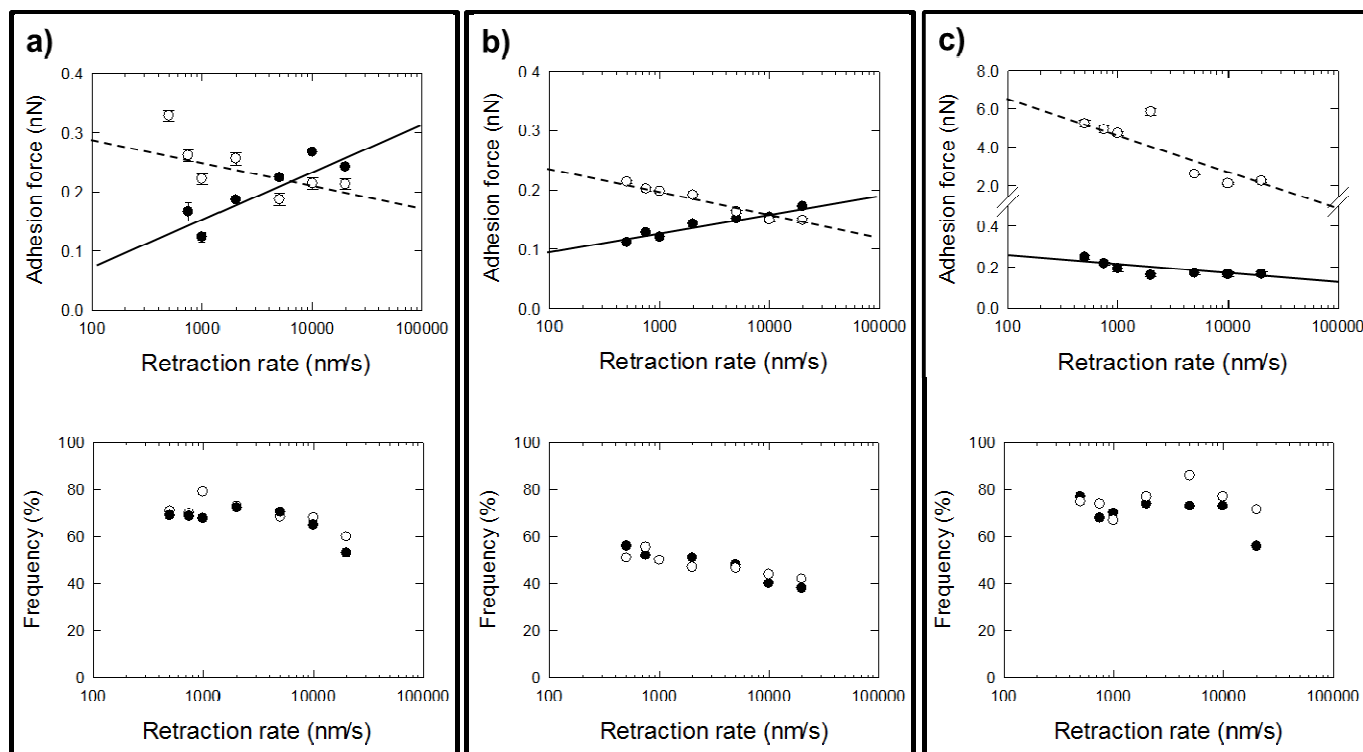
8

Figure 7.

Variations of the average adhesion force and the probability of adhesive events as a function of the retraction rate performed by force spectroscopy over 10 μm × 10 μm surface areas in aqueous medium at 37°C with the monovalent (black circle) and the tetravalent (white circle) adamantyl scaffold grafted on the AFM-tip. a) SAM-CD(NP) b) SAM-CD; c) PAH-CD coated gold substrate. Each mean value corresponds to the arithmetic mean of the non-zero forces out of the 3×1024 force curves recorded; the error bars correspond to the standard errors. All these force measurements were performed with an approach rate of 1000 nm/s, a loading force of 250 pN, and a contact time of 1s.

Graphical Abstract
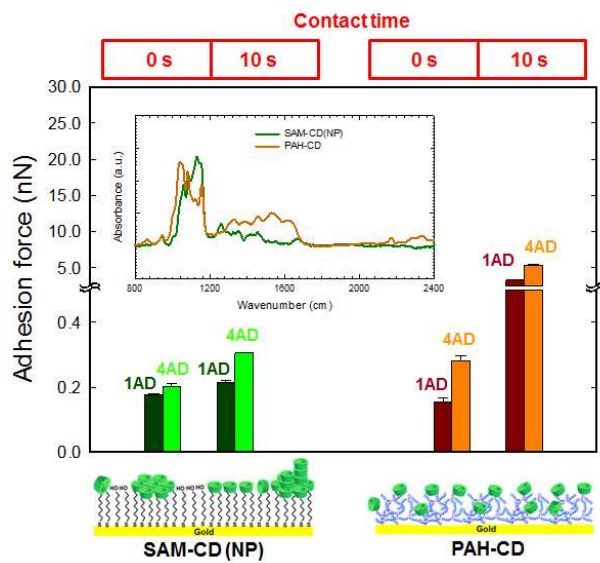
Molecular orientation and flexibility of β-CD modulate the contact time and the multivalence effects of specific host-guest interactions.